# Real time dielectric relaxation of poly(ethylene terephthalate) during crystallization from the glassy state

**T. A. Ezquerra and F. J. Baltà-Calleja***
*Instituto de Estructura de la Materia, CSIC, Serrano 119, Madrid 28006, Spain*

**and H. G. Zachmann**
*Institut für Technische und Makromolekulare Chemie, Hamburg University, Hamburg, Germany*
*(Received 28 May 1993; revised 18 November 1993)*

The crystallization of poly(ethylene terephthalate) has been followed in real time by measuring the dielectric complex permittivity. The measurements have been discussed by assuming the contribution to the dielectric losses of two types of amorphous phases: amorphous regions filling the interspherulitic space and amorphous regions located between crystalline lamellae within the spherulites. The deviation of the measurements from the calculated values assuming a simple two-phase model has been interpreted as being due to changes in the nature of the amorphous regions as crystallization proceeds. A phenomenological description of the experiments in terms of the Havriliak–Negami description permits the changes of the relaxation time distribution functions upon crystallization to be followed. The evolution with crystallization time of the derived dipole moment time correlation functions are discussed in the light of different models.

**(Keywords: dielectric relaxation; PET; crystallization)**

## INTRODUCTION

The influence of crystallinity on the molecular dynamics of polymers shows interesting aspects which can be investigated by dielectric spectroscopy[1–5]. The segmental motions of the polymeric chain, appearing at temperatures above the glass transition temperature ($T_g$), which give rise to the $\alpha$ relaxation, are strongly affected by the presence of crystalline domains[6]. On the other hand, local motions like those causing the $\beta$ relaxation are less influenced by crystallinity[2,6].

Poly(ethylene terephthalate) (PET) has been frequently used as a model system to study the influence of crystallinity on different physical properties[7–9]. This is due to the fact that PET can be either obtained in the amorphous state or with a controlled amount of crystallinity. In particular, dielectric relaxation in PET has been the subject of a large amount of research[6,9,10]. Both the relaxation time distribution function and the central relaxation time $\tau_0$ are modified as the crystallinity of the sample changes. Owing to the limitation imposed by the measuring time being comparable to the time of crystallization the majority of studies have been carried out on isothermally crystallized samples from the glassy state and then quenched. However, a few measurements have been already performed in real time for PET[9,11]. The use of impedance analysers[12] capable of measuring over several decades in frequency for measuring times of $<1$ min has allowed dielectric measurements during crystallization in real time to be carried out more readily[13]. In this paper we present dielectric relaxation measurements performed in real time as crystallization of PET proceeds from the glassy state.

## EXPERIMENTAL

Commercial samples of PET (Hoechst AG, Germany) were obtained in the form of amorphous films ($\sim 100\,\mu$m thick). Measurements of the dielectric complex permittivity ($\varepsilon^* = \varepsilon' - i\varepsilon''$) were performed in the $10^3$–$10^6$ Hz frequency range using a Hewlett–Packard impedance analyser (HP 4192A). Films were provided with circular gold electrodes (3 cm diameter) obtained by sputtering the metal in both free surfaces.

The specimens were placed between two gold-plated stainless steel electrodes. The dielectric cell was introduced in a home-made furnace operating in a temperature controlled air atmosphere. For isothermal crystallization measurements the sample was introduced in the furnace previously heated at the selected crystallization temperature ($T_c$) above the $T_g$ of PET ($T_g \approx 75$°C). Under these conditions a heating rate of $\approx 2$°C min$^{-1}$ was obtained. After reaching the selected $T_c$, $\varepsilon^*$ measurements were performed in the $10^3$–$10^6$ Hz frequency range as a function of the crystallization time. Each measurement required 40 s. In the range of $T_c$ values investigated the sample was heated up above $T_g$ for 15–17 min before the selected $T_c$ was reached. The experimental conditions were chosen to avoid significant precrystallization effects of the sample during the heating process on the basis of previous crystallization experiments performed with

* To whom correspondence should be addressed

0032-3861/94/12/2600–07

different techniques[7,14]. At the end of each crystallization experiment the sample was rapidly cooled down to room temperature.

## THEORETICAL

The description of dielectric relaxation in terms of the Havriliak–Negami (HN) empirical equation[15] for the dielectric permittivity $\varepsilon^*$ has been shown to be of great use in dealing with polymeric materials[2]. For the case in which two relaxation processes are involved it reads:

$$\varepsilon^* = (\Delta\varepsilon^*)_\alpha + (\Delta\varepsilon^*)_\beta + (\varepsilon_\infty)_\beta \tag{1}$$

with

$$\Delta\varepsilon^* = \frac{\varepsilon_0 - \varepsilon_\infty}{[1+(i\omega\tau_0)^b]^c} \tag{2}$$

for each relaxation process, where $\varepsilon_0$ and $\varepsilon_\infty$ are the relaxed and unrelaxed dielectric constant values, $\tau_0$ is the central relaxation time and $b$ and $c$ are parameters which describe the symmetric and the asymmetric broadening of the relaxation time distribution function, respectively. Equation (2) can be used to derive the corresponding analytical expressions of the real and imaginary part[15] which read:

$$\varepsilon' = (\varepsilon_0 - \varepsilon_\infty) r^{-c} \cos(c\psi) + \varepsilon_\infty \tag{3}$$

$$\varepsilon'' = (\varepsilon_0 - \varepsilon_\infty) r^{-c} \sin(c\psi) \tag{4}$$

with

$$r^2 = 1 + 2(\omega\tau_0)^b \cos(b\pi/2) + (\omega\tau_0)^{2b} \tag{5}$$

and

$$\tan\psi = \frac{(\omega\tau_0)^b \sin(b\pi/2)}{1+(\omega\tau_0)^b \cos(b\pi/2)} \tag{6}$$

The relaxation process can also be described in terms of a relaxation time spectrum[16] by using the equation:

$$\frac{\varepsilon^* - \varepsilon_\infty}{\varepsilon_0 - \varepsilon_\infty} = \int_{-\infty}^{\infty} \frac{F(\tau/\tau_0)}{1+i\omega\tau} \mathrm{d}\ln(\tau/\tau_0) \tag{7}$$

The associated relaxation time spectrum is given by:

$$F(\tau/\tau_0) = \frac{1}{\pi} \frac{(\tau/\tau_0)^{bc} \sin(c\theta)}{[(\tau/\tau_0)^{2b} + 2(\tau/\tau_0)^b \cos(\pi b) + 1]^{c/2}} \tag{8}$$

being:

$$\theta = \arctan\left|\frac{\sin(\pi b)}{(\tau/\tau_0)^b + \cos(\pi b)}\right| \tag{9}$$

In the case of two different processes ($\alpha$ and $\beta$) by considering that $\Delta\varepsilon_\alpha = \varepsilon_{0_\alpha} - \varepsilon_{\infty_\alpha}$ and $\Delta\varepsilon_\beta = \varepsilon_{0_\beta} - \varepsilon_{\infty_\beta}$ one obtains[16]:

$$\Delta\varepsilon_\alpha^* = \int_{-\infty}^{\infty} \Delta\varepsilon_\alpha \frac{F_\alpha(\tau/\tau_{0_\alpha})}{1+i\omega\tau_\alpha} \mathrm{d}\ln(\tau/\tau_{0_\alpha}) \tag{10}$$

and

$$\Delta\varepsilon_\beta^* = \int_{-\infty}^{\infty} \Delta\varepsilon_\beta \frac{F_\beta(\tau/\tau_{0_\beta})}{1+i\omega\tau_\beta} \mathrm{d}\ln(\tau/\tau_{0_\beta}) \tag{11}$$

By substituting the two last expressions into equation (1) we obtain for the complete relaxation process:

$$\frac{\varepsilon^* - \varepsilon_{\infty_\beta}}{\varepsilon_{0_\alpha} - \varepsilon_{\infty_\beta}} = \int_{-\infty}^{\infty} \frac{F_{\alpha+\beta}(\tau/\tau_{0_\alpha})}{1+i\omega\tau_\alpha} \mathrm{d}\ln(\tau/\tau_{0_\alpha}) \tag{12}$$

with

$$F_{\alpha+\beta}(\tau/\tau_{0_\alpha}) = \frac{\Delta\varepsilon_\alpha}{\varepsilon_{0_\alpha} - \varepsilon_{\infty_\beta}} F_\alpha(\tau/\tau_{0_\alpha}) + \frac{\Delta\varepsilon_\beta}{\varepsilon_{0_\alpha} - \varepsilon_{\infty_\beta}} F_\beta(\tau/\tau_{0_\beta}) \tag{13}$$

after considering that $\mathrm{d}\ln(\tau/\tau_{0_\alpha}) = \mathrm{d}\ln(\tau/\tau_{0_\beta})$.

It has been shown that the HN equation with two parameters, $b$ and $c$, describes satisfactorily frequency domain data in a great variety of systems. Recently, Schönhals and Schlosser proposed a model which relates the $b_\alpha$ parameter to large scale motions and the value of $c_\alpha b_\alpha$ to small scale motions[17]. Experimental evidence for the model has been presented for different systems including low molecular weight glass forming liquids and polymers[10,18,19].

The dielectric complex permittivity $\varepsilon^*$ is related to a relaxation function, $\phi(t)$ by a pure imaginary Laplace transformation[20–22] of the form:

$$\frac{\varepsilon^* - \varepsilon_\infty}{\varepsilon_0 - \varepsilon_\infty} = \mathscr{L}\left[-\frac{\mathrm{d}\phi(t)}{\mathrm{d}t}\right] = \int_0^\infty \exp(-i\omega t)\left[-\frac{\mathrm{d}\phi(t)}{\mathrm{d}t}\right]\mathrm{d}t \tag{14}$$

The knowledge of $\phi(t)$ over the entire time range makes it possible to derive values of $(\varepsilon^* - \varepsilon_\infty)/(\varepsilon_0 - \varepsilon_\infty)$. Inversely, it can be shown that:

$$\phi(t) = \frac{2}{\pi}\int_0^\infty \left(\frac{\varepsilon''(\omega)}{\varepsilon_0 - \varepsilon_\infty}\right)\cos(\omega t)\frac{\mathrm{d}\omega}{\omega} \tag{15}$$

The relaxation function $\phi(t)$ is approximately the same as the dipole moment time correlation function which has been related to the elemental dipole moment at a given time, $\mu_j(t)$, in a polymeric chain[21] by:

$$\phi(t) = \frac{\sum_i^N \sum_j^N \langle \mu_i(0)\mu_j(t)\rangle}{\sum_i^N \sum_j^N \langle \mu_i(0)\mu_j(0)\rangle} \tag{16}$$

Experimentally the shape of $\phi(t)$ has been described in terms of the stretched exponential function of Kohlrausch–Williams–Watts (KWW)[22]:

$$\phi(t) = a\exp[-(t/\tau_{\mathrm{KWW}})^\beta] \tag{17}$$

where $\tau_{\mathrm{KWW}}$ is a characteristic relaxation time and $\beta$ takes values between 0 and 1. The mean relaxation time with this representation is given by:

$$\langle\tau\rangle = \left[\frac{\tau_{\mathrm{KWW}}}{\beta}\Gamma\left(\frac{1}{\beta}\right)\right] \tag{18}$$

where $\Gamma$ is the Gamma function.

The KWW stretched exponential describes with a single parameter, $\beta$, time domain experiments. The relationship between the $b$ and $c$ parameters of the HN formulation, which describes a relaxation process in the frequency domain, and the corresponding $\beta$ parameter, which describes the same process in the time domain, is of great interest[23,24].

The coupling theory[25], which considers the material as composed of relaxing units coupled to a complex system, predicts a KWW stretched exponential function for the dipole moment autocorrelation function with $\beta = 1-n$. Here $n$ is a new parameter which indicates the degree of coupling.

## RESULTS

Dielectric loss ($\varepsilon''$) values corresponding to the initial amorphous sample are represented *versus* temperature for various frequencies in *Figure 1*. In accordance with

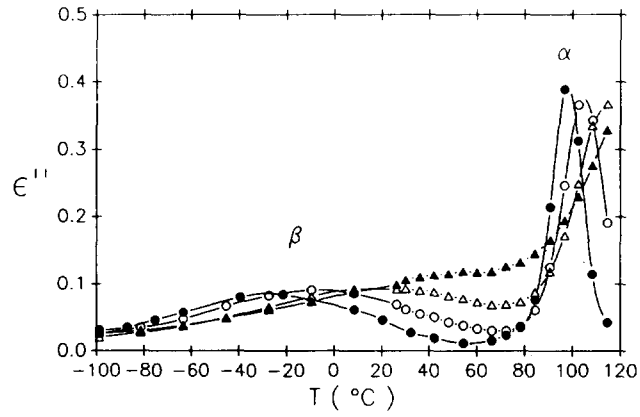


**Figure 1** Dielectric loss, $\varepsilon''$, for initial PET amorphous sample as a function of temperature at different frequencies: (●) $10^3$; (○) $10^4$; (△) $10^5$; (▲) $10^6$Hz

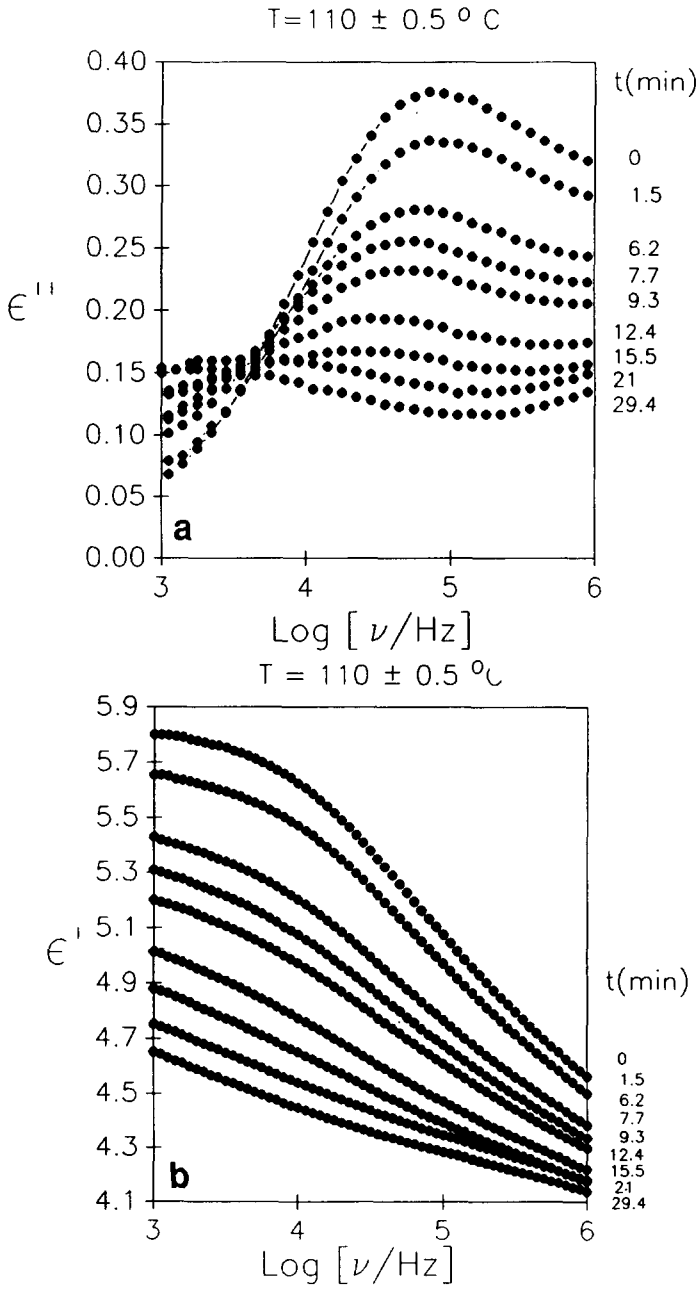


**Figure 2** (a) Real time evolution of the dielectric loss during isothermal crystallization ($T_c = 110$°C) as a function of frequency at selected crystallization times. (b) Real time evolution of the dielectric constant during isothermal crystallization ($T_c = 110$°C) as a function of frequency at selected crystallization times

previous studies[6] two main dielectric relaxations can be distinguished in this investigated temperature range: the lower temperature relaxation, $\beta$, due to the local motion of the –COO groups attached to both sides of the benzene ring[2,6,26]; and the higher temperature relaxation, $\alpha$, associated with long range motions appearing in the polymeric chain at temperatures above $T_g$. The real time variation of $\varepsilon''$ and $\varepsilon'$ with frequency at $T = 110$°C is illustrated in *Figures 2a* and *b* for different crystallization times. The values of the logarithm of the frequency of maximum loss, $\nu_{max}$, and the ratio $\varepsilon''_{max}(t)/\varepsilon''_{max}(0)$ have been represented as a function of the crystallization time for two selected temperatures in *Figures 3a* and *b*. The experimental error in the determination of both magnitudes is estimated as the size of the data points. It can be seen that the variation rate of both magnitudes becomes smaller as $T_c$ is reduced. Furthermore, at both temperatures the relative changes of $\varepsilon''_{max}$ and $\nu_{max}$ with time are different from each other. At the beginning of crystallization while $\nu_{max}$ stays constant $\varepsilon''_{max}$ immediately shows a clear decrease. According to *Figure 3b*, primary crystallization could be close to completion at ~20 min. However, while the intensity levels at this time, $\nu_{max}$ still continues shifting to smaller frequencies (*Figure 3a*).

## DISCUSSION

### *Dielectric relaxation in terms of a two-phase model*

The experiments carried out during the crystallization process of PET permit the changes of the molecular dynamics of polymer chains from the glassy state to be monitored in real time. It is known that PET crystallization from the glassy state gives rise to spherulitic

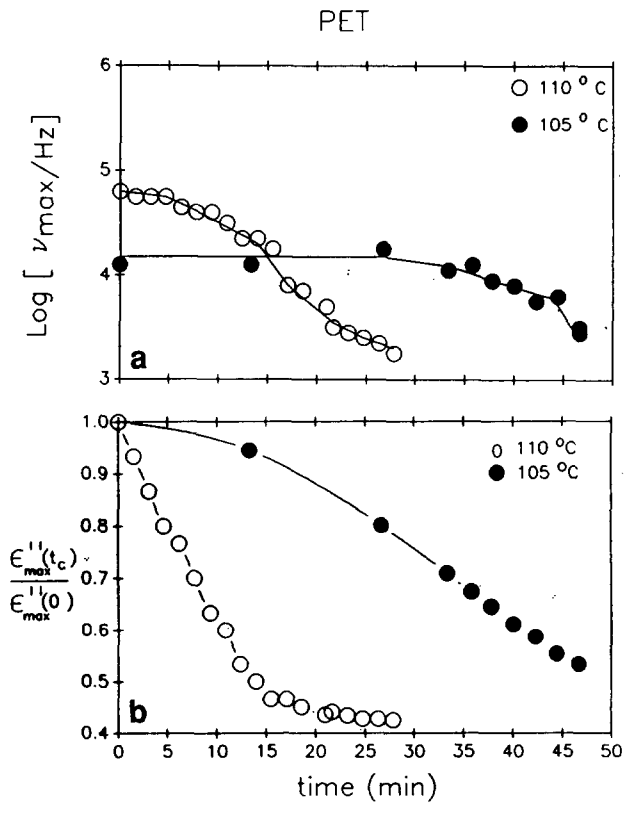


**Figure 3** (a) Relative variation of the frequency of maximum loss values, $\nu_{max}$, as a function of the crystallization time. (b) Relative variation of the maximum dielectric loss values, $\varepsilon_{max}(t)/\varepsilon_{max}(0)$, as a function of the crystallization time

morphologies[27,28]. At the crystallization temperatures investigated of 105 and 110°C there is a net decrease of amorphous material which is related to the $\varepsilon''_{max}$ decrease with time presented in *Figure 3b*. In addition, if one takes into account that $(2\pi\nu_{max})^{-1}$ is an average relaxation time[3], the observed decrease of $\nu_{max}$ in *Figure 3a* suggests a slowing down of the chain mobility as crystallization evolves.

For a more quantitative discussion we have to consider the mechanism of crystallization in more detail. It is generally accepted that during isothermal crystallization first spherulites or other morphological units are growing until they impinge on each other and fill the sample volume completely. This process is called primary crystallization. Each spherulite consists of lamellar stacks of crystals and amorphous regions. In addition to the growth of spherulites an increase of the degree of crystallization within the spherulites takes place. This process is called secondary crystallization. As first proposed by Tidy and Williams[3,11], dielectric relaxation of PET during primary crystallization can be qualitatively explained considering the influence of two different kinds of amorphous regions which coexist during primary crystallization: (i) the amorphous regions between the spherulites which are very large compared to the length of the molecules and, therefore, should not be very sensitive to the spherulite formation process. As a consequence, the dielectric loss curves arising from these regions should have similar shape to that corresponding to the completely amorphous material; (ii) the amorphous regions between the crystals within the spherulites. These regions consist of short chains, the ends of which are likely to be attached to the crystal surfaces.

According to *Figure 2a*, the loss curve at $t=0$ corresponding to the amorphous sample has its maximum at $63\times10^3$ Hz while that for the sample crystallized at 110°C for 21 min [which, according to the variation of $\varepsilon''_{max}(t)/\varepsilon''_{max}(0)$ in *Figure 3b*, can be considered to be filled almost completely by spherulites] has its maximum at $5\times10^3$ Hz. In addition, the curve of the crystallized sample ($t=21$ min) is broader than that of the amorphous sample. These differences can be attributed to the fact that the amorphous regions in the crystallized sample consist of short chains, the ends of which are attached to the crystal surfaces. Furthermore, the volume available to these chains is restricted by the neighbouring crystals; usually these amorphous regions have a thickness of only 5–10 nm. All these factors restrict the mobility and cause a shift of the maximum to lower frequencies. As these restrictions may strongly vary from chain to chain the curve also becomes broader.

In order to test quantitatively the validity of the above two-phase model we can consider, based on the Onsager equation[29], to a first approximation that:

$$\varepsilon'' = \Phi\varepsilon''_{as_{final}} + (1-\Phi)\varepsilon''_a \qquad (19)$$

where $\Phi$ is the mass fraction of amorphous material in the spherulites normalized to the total amount of amorphous material, and $\varepsilon''_{as_{final}}$ and $\varepsilon''_a$ are contributions of the intraspherulitic and interspherulitic amorphous regions, respectively.

*Figure 4* shows the dielectric loss curves generated by application of equation (19) after considering the initial curve at $t=0$ as $\varepsilon''_a$ and the curve at $t=21$ as $\varepsilon''_{as_{final}}$ and changing the parameter $\Phi$. By comparing the calculated ratio $\varepsilon''_{max}(\Phi)/\varepsilon''_{max}(0)$ with the experimental values of

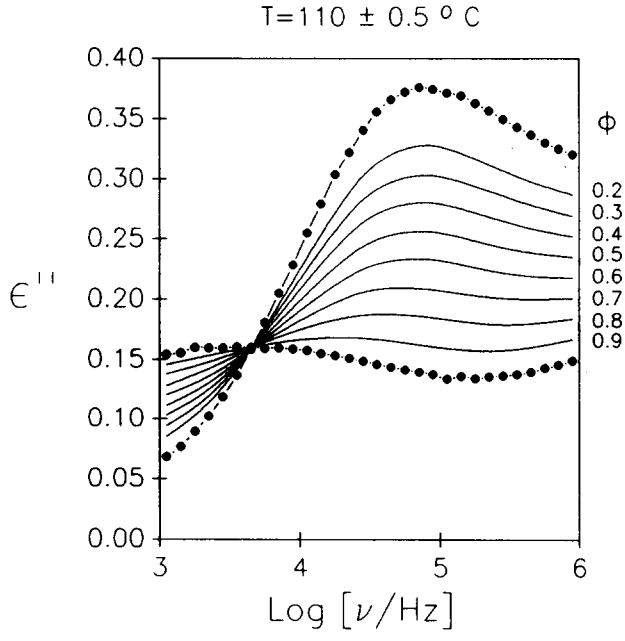


**Figure 4** Dielectric loss curves generated according to the two-phase model [equation (19)] (—). Data for the upper and lowest values correspond to the two limiting loss curves (see text). $\Phi$ parameter is the relative fraction of amorphous material within the spherulites

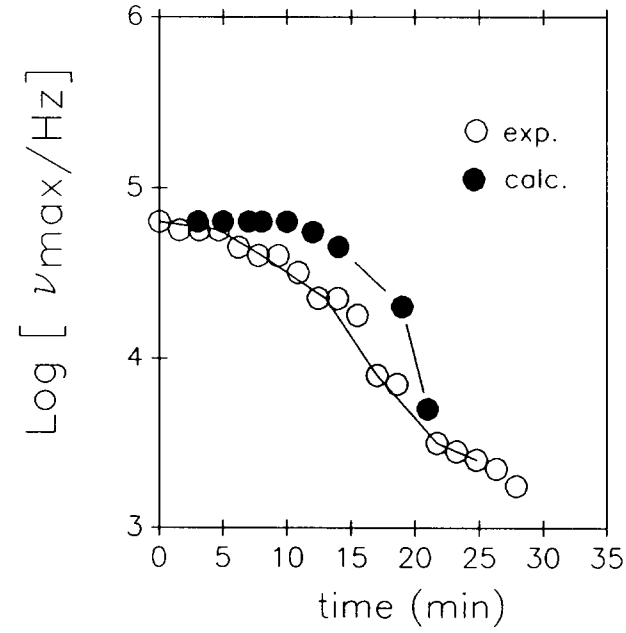


**Figure 5** Calculated $\nu_{max}$ values according to the two-phase model and experimental $\nu_{max}$ values

*Figure 3b* an estimation of the crystallization time can be made. The existence in *Figure 4* of an isosbestic frequency at which $\varepsilon''$ is independent of $\Phi$ is a consequence of the assumption that the contribution of the amorphous regions within the spherulites at a given time, $\varepsilon''_{as}$, coincides with $\varepsilon''_{as_{final}}$. The absence of such an isosbestic frequency in the experimental values of $\varepsilon''$ shown in *Figure 2a* seems to indicate that $\varepsilon_{as}$ is time-dependent. Comparison of the calculated and experimental $\nu_{max}$ values as a function of the crystallization time is shown in *Figure 5*.

One can see that, with increasing time, the measured $\nu_{max}$ data gradually shift to smaller values whereas the calculated ones remain constant up to almost the end of crystallization. From this we conclude that the shape of

the loss curve arising form the amorphous regions within the spherulites, $\varepsilon''_{as}$, is not the same at all times and, in particular, is not identical with the shape of $\varepsilon''_{as_{final}}$. Instead, in order to generate the measured curves one has to assume that the maximum of the curve $\varepsilon''_{as}$ shifts to lower frequencies with increasing time. In other words, this result suggests that during the initial stages of crystallization, the appearance of incipient spherulitic domains does not significantly disturb the average chain mobility in the amorphous phase. Only after the crystalline phase has achieved a significant volume fraction, is the material in the amorphous phase affected by the rigid molecules of the crystalline phase.

How can this shift of $\nu_{max}$ be explained? If the amorphous regions between the crystals within the spherulites were very large, the mobility of the chains in these regions would not be influenced by the presence of the crystals and $\varepsilon''_{as}$ would have the same shape as $\varepsilon''_{a}$. The smaller these regions become the more restricted is the mobility of the chains and, as a consequence, the smaller becomes the value of $\nu_{max}$ at which the maximum of $\varepsilon''_{as}$ appears. Therefore, we conclude that at the beginning of crystallization the distances between the neighbouring crystals within the spherulites is comparatively large. With increasing time, new crystals are formed between the already existing ones (secondary crystallization) and the amorphous regions thus become smaller. This model for the process of crystallization corresponds to the view proposed by Schultz[30] according to which 'loose' spherulites are first formed and become 'dense' spherulites in later stages of crystallization. Such a model is also supported by our previous investigations involving simultaneous measurements of wide- and small-angle X-ray scattering during isothermal crystallization of PET[31].

*Dielectric relaxation in terms of the phenomenological description of Havriliak and Negami*

The HN approximation, which has been previously applied to isothermally crystallized PET[6], has been used here in an attempt to describe the present real time experiments. However, due to the fact that the experimental frequency range does not cover, at the $T_c$ of interest, the complete $\beta$ relaxation process, this must be simulated in order to fit the $\varepsilon^*$ experimental data to equation (2). The extrapolation procedure of Coburn and Boyd has been employed[6] to fit the results shown in *Figures 2a* and *b*. The parameters characterizing the $\beta$ relaxation process for the PET amorphous sample were fitted to equation (2) for the lower temperature region. Then by assuming that these parameters are linearly dependent on temperature they were extrapolated to higher temperatures. This procedure was performed for the initial amorphous sample and for the same sample after the crystallization experiment. In this way the parameters of the $\beta$ process can be directly obtained for the initial and final crystallization time. For crystallization times in between, the fitting parameters were allowed to vary between the limiting values obtained. A subroutine based on the Newton method[32] was modified to fulfil our requirements and used in the fitting under the condition $\varepsilon_{0_\beta} = \varepsilon_{\infty_\alpha}$.

*Figure 6* shows the evolution with time of the dielectric relaxation in the form of Cole–Cole plots during crystallization. The continuous lines correspond to the calculated fittings according to equation (1) where the

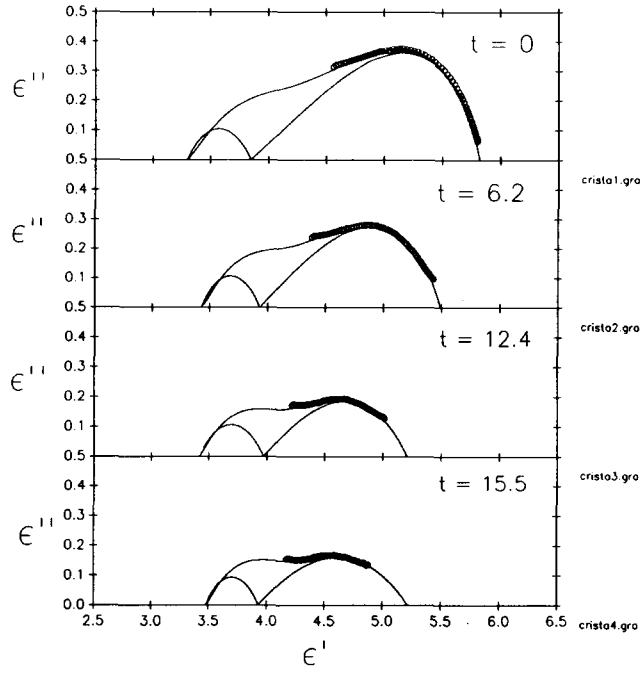


**Figure 6** Cole–Cole plots for selected crystallization times at $T_c = 110°C$. Solid curves denote calculated values according to equations (1)–(6) and represent the separated and total contribution of the $\beta$ (left) and $\alpha$ (right) relaxation process

**Table 1** $\Delta\varepsilon_\alpha$, $b_\alpha$, $c_\alpha$ and $(\tau_0)_\alpha$ obtained from the fitting of equation (1). The extrapolated parameters corresponding to the $\beta$ process are denoted by $\Delta\varepsilon_\beta$, $b_\beta$ and $(\tau_0)_\beta$

| $t$(min) | $\Delta\varepsilon_\alpha$ | $b_\alpha$ | $c_\alpha$ | $(\tau_0)_\alpha$ | $\Delta\varepsilon_\beta$ | $b_\beta$ | $(\tau_0)_\beta$ |
|---|---|---|---|---|---|---|---|
| 0 | 1.97 | 0.74 | 0.30 | $8.83\times10^{-6}$ | 0.55 | 0.46 | $1.89\times10^{-9}$ |
| 6.2 | 1.56 | 0.61 | 0.41 | $1.05\times10^{-5}$ | 0.51 | 0.51 | $2.7\times10^{-9}$ |
| 12.4 | 1.24 | 0.45 | 0.57 | $2.29\times10^{-5}$ | 0.55 | 0.47 | $2.5\times10^{-9}$ |
| 15.5 | 1.29 | 0.34 | 0.75 | $2.46\times10^{-5}$ | 0.45 | 0.51 | $4.6\times10^{-9}$ |

individual $\alpha$ and $\beta$ relaxation processes have been also represented. The corresponding parameters are shown in *Table 1*. For the initial amorphous sample at $t=0$ (i.e. after reaching $T_c$ from room temperature at a heating rate of $\approx 2°C\,min^{-1}$) results are in good agreement with those previously reported[6,10] for amorphous PET. This result indicates the absence of significant crystallization during the initial heating process. It is noteworthy that the dielectric strength $(\Delta\varepsilon)_\alpha$ decreases and the central relaxation time $(\tau_0)_\alpha$ increases as crystallization proceeds. On the other hand, the squeezing parameter $c_\alpha$ increases from 0.3 to 0.75 as a function of crystallization time.

It is interesting to compare the relaxation strength of the amorphous region and of the crystalline sample. According to *Table 1*, $(\Delta\varepsilon)_\alpha$ is reduced to ~65% after crystallization for 15.4 min. From corresponding density measurements it is known that the amorphous fraction of a sample crystallized under such conditions only decreased to 75%. From this it follows that the fraction of less mobile chains is higher than those forming the crystalline phase. Similar results have been obtained by other authors[3,9].

In order to follow the change of the dipole moment time correlation function corresponding to the $\alpha$ process, equation (15) has been numerically solved. The $\varepsilon''(\omega)$ values were generated from equations (4), (5) and (6) considering the $c_\alpha$ and $b_\alpha$ parameters corresponding to

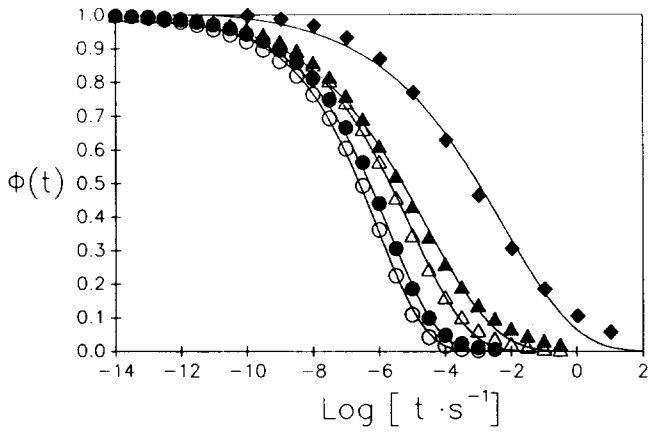


**Figure 7** Normalized dipole moment time correlation function, $\phi(t)$ (symbols) and best fit (*Table 2*) to a KWW stretched exponential (solid lines) corresponding to the crystallization times of *Figure 6*: (○) 0; (●) 6.2; (△) 12.4; (▲) 15.5 min. The ◆ values correspond to $b_\alpha = 0.28$ and $c_\alpha = 1$. $\tau_0 = 1 \times 10^{-3}$ values were taken from reference 6 (see text). The best fit to a KWW stretched exponential for this case gives $\beta = 0.19$

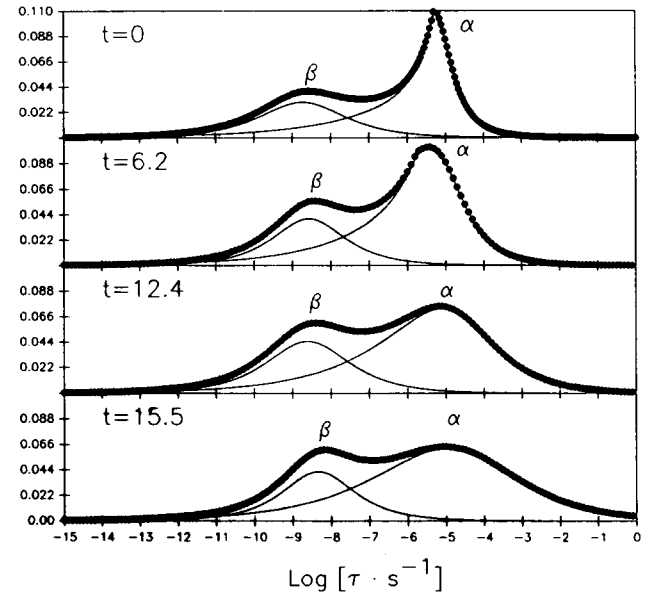


**Figure 8** Distribution of relaxation times of PET ($T_c = 110°C$) at the labelled crystallization times

**Table 2** Fitting parameters $\beta$ and $\tau_{KWW}$ corresponding to the KWW stretched exponential and calculated [equation (18)] mean relaxation time $\langle\tau\rangle$

| $t$ (min) | $\beta$ | $\tau_{KWW}$ | $\langle\tau\rangle$ |
|---|---|---|---|
| 0 | 0.3 | $9 \times 10^{-7}$ | $8.3 \times 10^{-6}$ |
| 6.2 | 0.29 | $1.9 \times 10^{-6}$ | $2 \times 10^{-5}$ |
| 12.4 | 0.25 | $9.4 \times 10^{-6}$ | $2.2 \times 10^{-4}$ |
| 15.5 | 0.21 | $2.9 \times 10^{-5}$ | $2.3 \times 10^{-3}$ |

each crystallization time (*Table 1*). A subroutine based on the Hagenah procedure[23] was developed to solve equation (15). The normalized $\phi(t)$ functions for the $\alpha$ process corresponding to the different crystallization times are represented in *Figure 7* as a function of $\log t$. The continuous lines correspond to the best fit of the obtained values to the KWW function. The corresponding fitting parameters are shown in *Table 2*. The mean relaxation times obtained by means of equation (18) are presented in the last column of *Table 2*.

From the HN analysis it is seen that as crystallinity increases a modification of the $\alpha$ relaxation time distribution function occurs. The total distribution time relaxation function, calculated according to equation (13), is shown in *Figure 8* for each selected crystallization time using the parameters reported in *Table 1*. The distribution functions include the $\beta$ relaxation, at shorter times, and the $\alpha$ relaxation at longer times. For the initial crystallization time the distribution of relaxation times for the $\alpha$ process is strongly asymmetric, as derived from the low value of the $c_\alpha$ squeezing parameter, in agreement with other authors[6,10]. As crystallinity increases the distribution of relaxation times becomes broader and tends to be more symmetric as revealed by the decrease of the $b_\alpha$ value and the concurrent increase of the $c_\alpha$ value, respectively. For semicrystalline PET samples a value of $c_\alpha = 1$ has been reported[6,10].

According to the model of Schlosser and Schönhals[10], the observed decrease of $\alpha_\alpha$ could be interpreted as due to the increasing hindrance for large scale motions as crystallization occurs and progressively the system is being covered by spherulites. On the other hand, as can be derived from *Table 1*, the value of $c_\alpha b_\alpha$ does not change significantly. This would imply that small scale motions are less affected by the crystallization process.

*The $\beta$ parameter of the KWW function*

As shown in *Figure 7*, the dipole moment time correlation function is also affected by the crystallization process. The $\phi(t)$ function can be well described in terms of the KWW function although systematic deviations are observed at higher times as crystallinity increases. The mean relaxation time calculated from equation (18) increases indicating, thus, the progressive slowing down of the polymeric changes as crystallinity evolves. For comparison the $\phi(t)$ function has been calculated for data reported in the literature for an isothermally crystallized PET sample ($T_c = 115°C$, $t_c = 20$ h)[6]. The same systematic deviation at higher times is observed.

It has been shown that there are a set of couples $b$, $c$ from the HN formulation which are related to a single $\beta$ stretching parameter from the KWW function[24]. The question arises as to whether the couple of HN parameters which describe the $\alpha$ relaxation in semicrystalline polymers can be described with a unique $\beta$ parameter in the time domain as well as it seems to occur in amorphous polymers[33]. Irrespective of this one can use the corresponding $\beta$ parameter in a qualitative discussion.

The calculated $\beta$ parameter decreases as crystallization proceeds. According to the coupling theory, proposed by Ngai *et al.*[25], a decrease of the $\beta = 1 - n$ parameter can be interpreted as a strengthening of the coupling between the relaxing species and the medium and seems to be related to an overall decrease of the molecular mobility[34]. Such a decrease of the $\beta$ parameter has been observed in polymeric systems at the liquid to glass transition[34]. In our case the observed $\beta$ decrease can be qualitatively interpreted, in a similar way, as being due to the progressively higher coupling between the remaining polymeric chains in the amorphous phase and the semicrystalline system as crystallinity develops.

## CONCLUSIONS

Dielectric relaxation measurements can be used to characterize the changes occurring in PET during

isothermal crystallization. A two-phase model based on the separated contribution of intraspherulitic and interspherulitic amorphous phases allows experiments to be described qualitatively. The changes in the nature of the two amorphous regions provoking the evolution from loose to more densely packed spherulites, due to secondary crystallization, must be considered in a quantitative discussion. The changes observed in the dielectric relaxation process during crystallization can be phenomenologically described in terms of the HN equation. The relaxation time distribution function reveals changes from a strongly asymmetric distribution towards a broad and symmetric distribution as crystallization proceeds. This evolution has been interpreted as due to a restriction of long scale motions of the polymeric chains as the material is filled in with spherulites. The dipole moment time correlation functions can be well described as KWW functions. The increase of the mean relaxation time suggests a progressive reduction of overall mobility of the polymeric chains as the system becomes more crystalline. The increase of the stretching of the dipole moment time correlation function can be qualitatively interpreted, in terms of the coupling model, as due to an increase of the coupling between the relaxing species in the amorphous phase and the whole system.

## ACKNOWLEDGEMENTS

The encouraging and fruitful comments made by G. Williams and F. Kremer are gratefully acknowledged. Thanks are due to CICYT Spain (Grant MAT-90-0795) for supporting this investigation and to the Alexander von Humbolt Stiftung for generously supporting the work within the scheme 'Research Cooperation Europe'.

## REFERENCES

1 McCrum, N. G., Read, B. E. and Williams, G. 'Anelastic and Dielectric Effects in Polymeric Solids', Dover Publishers Inc., New York, 1991
2 Hedvig, P. 'Dielectric Spectroscopy of Polymers', Adam Hilger Ltd, Bristol, 1977
3 Williams, G. *Adv. Polym. Sci.* 1979, **33**, 59
4 Ashcraft, C. R. and Boyd, R. H. *J. Polym. Sci., Polym. Phys. Edn* 1976, **14**, 2153
5 Sandrolini, F., Motori, A. and Saccani, A. *J. Appl. Polym. Sci.* 1992, **44**, 765
6 Coburn, J. C. and Boyd, R. H. *Macromolecules* 1986, **19**, 2238
7 Santa Cruz, C., Baltá Calleja, F. J., Zachmann, H. G., Stribeck, N. and Asano, T. *J. Polym. Sci., Polym. Phys. Edn* 1991, **29**, 819
8 Santa Cruz, C., Stribeck, N., Zachmann, H. G. and Baltá Calleja, F. J. *Macromolecules* 1991, **24**, 5980
9 Sawada, K. and Ishida, Y. *J. Polym. Sci., Polym. Phys. Edn* 1975, **13**, 2247
10 Schlosser, E. and Schönhals, A. *Colloid Polym. Sci.* 1989, **267**, 963
11 Tidy, D. and Williams, G. unpublished results
12 Kremer, F., Boese, D., Meier, G. and Fischer, E. W. *Progr. Colloid Polym. Sci.* 1989, **80**, 129
13 Nowak, H., Kalinka, G. and Hinrichsen, G. *Acta Polym.* 1993, **44**, 25
14 Baltá-Calleja, F. J., Santa Cruz, C. and Asano, T. *J. Polym. Sci., Polym. Phys. Edn* 1993, **31**, 557
15 Havriliak, S. and Negami, S. *Polymer* 1967, **8**, 161
16 Böttcher, C. J. F. and Bordewijk, P. 'Theory of Electric Polarization', Vol. 2, Elsevier, Amsterdam, 1978, p. 45
17 Schönhals, A. and Schlosser, E. *Colloid Polym. Sci.* 1989, **267**, 125
18 Schlosser, E. and Schönhals, A. *Colloid Polym. Sci.* 1989, **267**, 133
19 Schönhals, A., Kremer, F. and Schlosser, E. *Phys. Rev. Lett.* 1991, **67**, 999
20 Cook, M., Watts, D. C. and Williams, G. *Trans. Faraday Soc.* 1970, **66**, 2503
21 Williams, G. *Chem. Rev.* 1972, **72**, 1, 55
22 Williams, G. and Watts, D. C. *Trans. Faraday Soc.* 1970, **66**, 80
23 Boese, D., Momper, B., Meier, G., Kremer, F., Hagenah, J. U. and Fischer, E. W. *Macromolecules* 1989, **22**, 12, 4416
24 Alvarez, F., Alegria, A. and Colmenero, J. *Phys. Rev. B* 1991, **44**, 14, 7306
25 Ngai, K. L., Rajagopal, A. K. and Teiler, S. *J. Chem. Phys.* 1988, **88**, 5086
26 Illers, K. H. and Breuer, H. *J. Colloid Sci.* 1963, **18**, 1
27 Zachmann, H. G. and Stuart, H. *Makromol. Chem.* 1960, **41**, 731
28 Groeninckx, G. and Reynaers, H. *J. Polym. Sci., Polym. Phys. Edn* 1980, **B18**, 1325
29 Böttcher, C. J. F. and Bordewijk, P. 'Theory of Electric Polarization', Vol. 1, Elsevier, Amsterdam, 1973, p. 258
30 Schultz, J. M. *Makromol. Chem. Makromol. Symp.* 1988, **15**, 339
31 Zachmann, H. G. and Wutz, C. in 'Crystallization of Polymers', NATO ASI Series (Ed. M. Dosier), Kluwer, Dordrecht, 1993, p. 403
32 Ebert, K., Ederer, H. and Isenhour, T. L. 'Computer Applications in Chemistry', VCH, Weinheim, 1989
33 Boyd, R. H., Devereaux, R. W. and Thayer, R. B. *Polym. Prepr.* 1990, **31**, 1, 279
34 Colmenero, J. *J. Non-Cryst. Solids* 1991, **131–133**, 860